Desalination and Water Treatment
www.deswater.com
doi: 10.1080/19443994.2014.940641

55 (2015) 2868–2883
August

Taylor & Francis
Taylor & Francis Group

Design of power systems for reverse osmosis desalination in remote communities

Amy M. Bilton[a,*], Leah C. Kelley[b]

[a]*Department of Mechanical and Industrial Engineering, University of Toronto, Toronto, ON, Canada, Tel. +1 617 7449785; email: bilton@mie.utoronto.ca*
[b]*Department of Mechanical Engineering, Massachusetts Institute of Technology, Cambridge, MA, USA*

Received 1 April 2014; Accepted 16 June 2014

ABSTRACT

Many remote communities lack access to a reliable water supply. They often have access to brackish groundwater or seawater, making reverse osmosis desalination a possible solution. However, reverse osmosis desalination is an energy-intensive process and many remote communities are off the electrical grid. Determining the most economic reverse osmosis system configuration and electrical power source for a given remote community is a challenge due to their unique resource availabilities. This paper presents an optimization-based approach to compare the economics of different small-scale reverse osmosis systems and power sources for remote communities. In this approach, physical models describe the performance of electrical power systems composed of photovoltaics, wind turbines, diesel generators, batteries, and hybrid systems. These power system models are coupled to a reverse osmosis system model to determine the water production. An optimization is performed to determine the most economic power system configuration, reverse osmosis system size, and water storage size that meets the desired water production reliability. The reliability is expressed as loss of water probability, which is computed using hourly environmental data. Here, this method is used to configure a reverse osmosis system for small communities. Results are presented for locations in Honduras, Eritrea, and Australia. Results show that the local climatic conditions greatly influence the economic attractiveness of different technologies. The variety of solutions found using this approach demonstrate the ability of the method to aid in the design of a power system and reverse osmosis system configuration for any location.

Keywords: Renewable energy; Reverse osmosis; System design; Optimization

*Corresponding author.

Presented at the Conference on Desalination for the Environment: Clean Water and Energy 11–15 May 2014, Limassol, Cyprus

1. Introduction

1.1. Motivation

Water access is a major challenge for many remote communities. Currently, 780 million people lack access to an improved water supply [1]. Many of these people live in small villages and communities off of the main water network. Fortunately, many of these locations have access to seawater or brackish groundwater making desalination a potential solution to their water issues.

There is a broad range of potential desalination solutions. These processes can be divided into two groups: thermal processes and membrane processes. Membrane processes include reverse osmosis, where water is forced through a membrane using a pressure higher than the osmotic pressure, leaving behind concentrated brine. In thermal processes, a phase change is used to make fresh water. Reverse osmosis desalination is well suited for small and medium remote communities due to its scalability and energy efficiency.

Despite the fact that reverse osmosis desalination has the lowest specific energy requirements of the developed desalination technologies, it still requires a significant amount of energy. Providing this energy is a significant challenge as many remote communities lack access to basic electricity [2]. Many of these communities rely on diesel generators to supply electricity which have high operating costs and pollute the environment. Using renewable sources to power reverse osmosis desalination, systems can lead to lower water costs and reduced environmental impact. Unfortunately, determining the best energy source and reverse osmosis system sizing is a challenge as each community has unique environmental conditions.

This paper presents a method to configure a cost-effective power system, size a reverse osmosis unit, and determine an appropriate water storage capacity to provide water for small remote communities. The method considers solar photovoltaics, wind, diesel generators, and hybrid combinations. A simulation model is used to analyze the performance of each energy system under local climatic conditions and its ability to meet the desalination power requirements. The method also uses a cost model to analyze the water cost associated with a given power system. The models are coupled to an optimization framework to determine the best energy mix and reverse osmosis system scale to meet the needs of individual locations. The approach is implemented for several locations and is shown to effectively select different systems tailored for the local renewable resources.

1.2. Background

The concept of coupling reverse osmosis systems to renewable energy sources is not new. Photovoltaic and wind-powered reverse osmosis systems have been designed and tested in a range of environments. Many of these systems are comprised of the renewable energy source, batteries, and a reverse osmosis system which is designed to operate at a constant set point. Using this concept, the Canary Islands Technological Institute developed a small battery-based photovoltaic reverse osmosis (PVRO) system [3,4]. Battery-based PVRO systems have also been commercialized by Spectra Watermakers [5]. Hybrid solar/wind reverse osmosis systems have been developed [6–8]. Researchers have also developed batteryless reverse osmosis systems powered by photovoltaics [9–12] or wind [13]. The different solutions developed show a large range of possible system configurations. A tool to determine which solution is most economical for a given location can help guide designers in configuring solutions, which are appropriate for local climatic conditions.

Methods for configuring renewable-powered reverse osmosis systems have been developed. Researchers have analyzed the feasibility of PVRO systems and have compared their economic feasibility with diesel reverse osmosis systems [14,15]. In both cases, PVRO systems were considered more economic in regions with good solar resources. Researchers have also looked at developing design tools to aid the design of power systems for reverse osmosis systems. Mohamed presents a method to design a hybrid PV and wind-powered RO system using a spreadsheet model and average solar and wind data to size the individual system components [9]. Voivontas describes a design program to aid in the design of a renewable energy-powered desalination system [16]. The software tool sizes the energy system and performs a financial analysis based on user inputs, and allows users to analyze different options. Bourouni et al., developed a method to optimize a renewable energy-powered RO system that considers photovoltaics and wind energy as possible power sources [17]. Their software sizes the components and simulates the system operations over a typical year to determine if the configurations are feasible. Though these works share similarities to the work proposed here, none of the methods incorporate optimization approaches and consider additional energy sources such as diesel generators.

Researchers have developed optimization approaches to couple renewable energy sources with reverse osmosis desalination systems [18]. In this

approach, a reverse osmosis system powered by photovoltaics, wind generators, and batteries is designed. The method uses genetic algorithms to configure a system that minimizes the water cost and meets the demand of the communities. The method segments the problem and determines the desalination system to meet the needs of a community then determines the renewable energy system to meet the desalination system's energy requirements. However, the size of the reverse osmosis system and its performance when paired with a renewable energy system are directly coupled. In this paper, these variables are simultaneously optimized to determine the best overall system for a given location. In addition, this paper considers hybrid configurations that include diesel generators.

2. Approach

2.1. Overview

A method for evaluating different configurations of off-grid reverse osmosis desalination systems is presented in this paper. In this method, different power systems and reverse osmosis systems are configured to provide water for a given community. The power systems considered here include photovoltaic panels with/without batteries, wind turbines with/without batteries, diesel generators, and hybrid combinations. Each configuration is evaluated and the most economic option is selected for each location.

The relative size of the components for each off-grid reverse osmosis desalination system is determined using the optimization structure shown in Fig. 1. An optimizer is coupled with a simulation model and cost model to evaluate each configuration. The simulation model uses hourly weather data for five years to evaluate the system reliability. Each hour, an energy balance is performed to determine the battery charge and the amount of water produced by the reverse osmosis system. Similarly, a water balance is performed each hour to determine the amount of water in storage. The reliability represents the amount of time that the system is able to meet the community water demand. Another model is used to estimate the lifecycle cost of each configuration. An optimizer uses these models to determine the system configuration that minimize the lifecycle cost subject to reliability constraints.

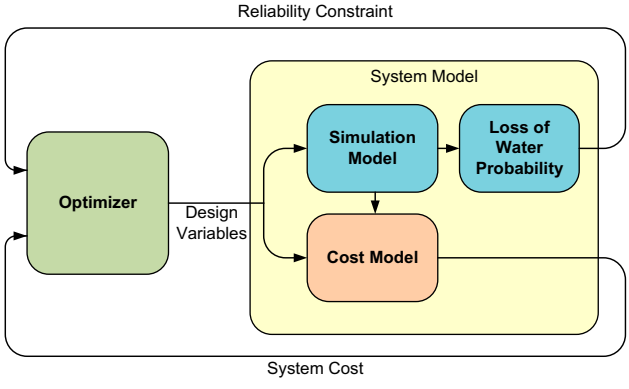

Fig. 1. Optimization framework.

For cases with continuous design variables, such as the PVRO systems with/without batteries, or the diesel-powered reverse osmosis system, the optimization algorithm selected is the Nelder–Mead simplex method. This technique was selected since it does not require gradient information, accommodates the discrete constraint function, and converges quickly for the small number of problem variables. A genetic algorithm was utilized for the larger optimization problems with discrete design variables. Despite the longer optimization time, this technique was chosen since it is a global optimization technique and it accommodates the discrete design variables.

2.2. Simulation model

The different power systems and reverse osmosis systems are simulated using the framework outlined in Fig. 2. The simulation is conducted using an hourly time step over a five-year window. The five-year simulation period was selected to provide adequate weather variations to analyze the system reliability. All simulations were conducted using a custom MATLAB script. Details of all subsystem models are presented in Section 3.

During each hour, an energy balance is completed on the power system. The amount of energy generated over the one-hour window is calculated from the solar radiation data, wind speed data, and diesel generator size. Similarly, the amount of energy required for the reverse osmosis desalination is calculated. Excess energy is stored in the batteries or an energy deficit is drawn from the batteries. If the batteries are depleted, the amount of available energy is put directly into producing water. This step assumes that the amount of water produced is proportional to the energy available.

Also, during each hour, a water balance is performed on the water tank. The amount of water produced by the reverse osmosis system is compared with the amount of water required by the community. Any excess is stored in the water tank and any deficit is drawn from the water tank. If there is insufficient

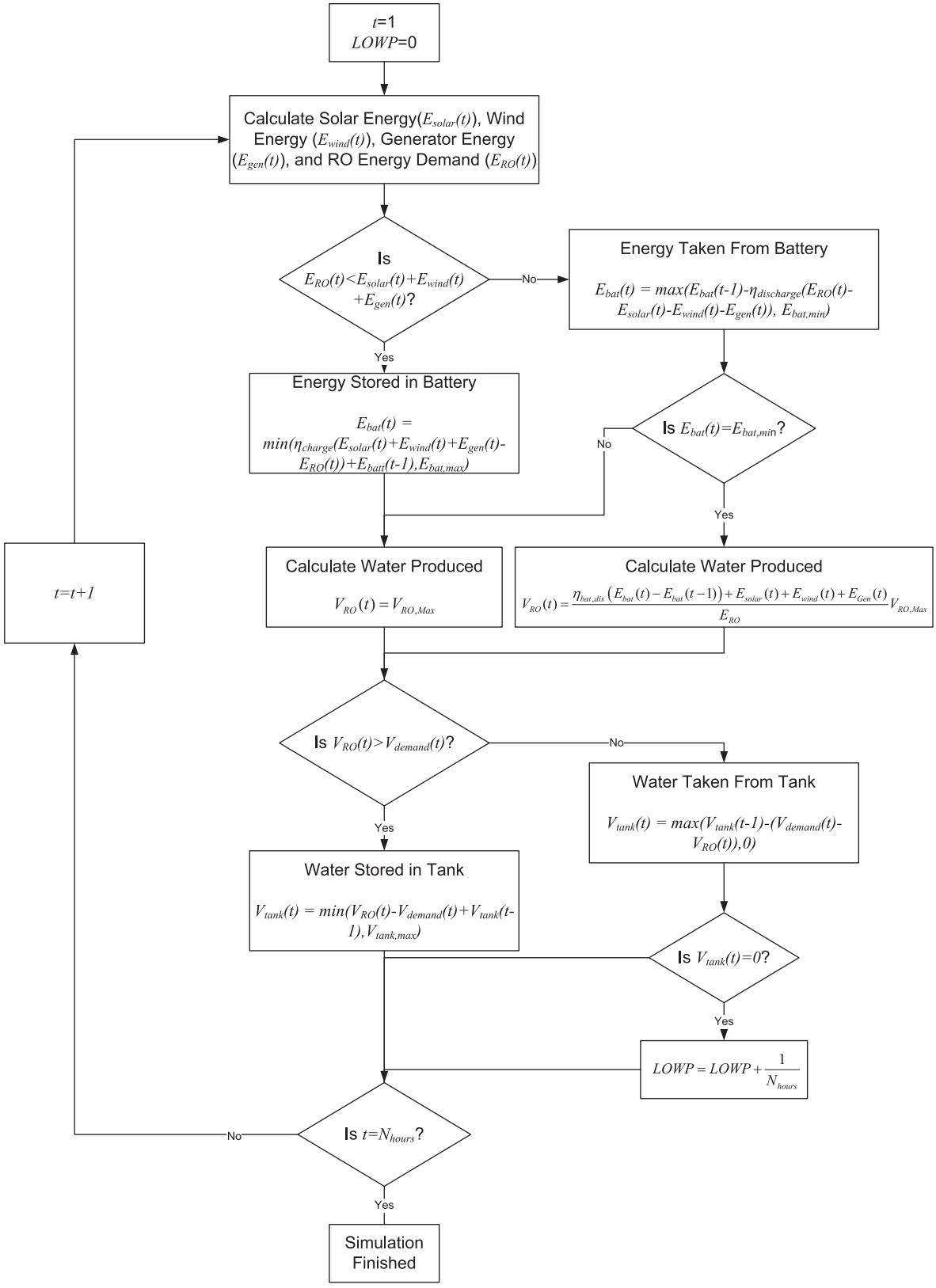

Fig. 2. Simulation model framework.

water in the tank to meet the demand, the period is counted to calculate the reliability of the system. Here, the reliability metric used is the loss of water probability and it is defined as:

$$LOWP = \frac{N_{\text{unmet}}}{N_{\text{hours}}} \tag{1}$$

where N_{unmet} is the number of hours in the simulation that the demand is not met and N_{hours} is the total number of hours in the simulation.

2.3. Cost model

The lifecycle cost is analyzed for each power and reverse osmosis system combination. Several metrics can be used to compare system economics, including average annual costs, cost per unit of water produced, or total lifecycle costs. Here, the net present value of the total system lifetime cost is used.

The total system lifetime cost, C_{LC}, is the sum of the net present values of the capital cost, C_{Cap}, operating and maintenance cost, $C_{O\&M}$, fuel cost, C_F, and carbon tax, C_{CT}, minus any alternative energy incentive and income tax credit, C_I:

$$C_{LC} = C_{Cap} + C_{O\&M} + C_F + C_{CT} - C_I \tag{2}$$

Renewable energy credits and carbon taxes are constantly changing and vary by location. Hence, they are set to zero here. Similarly, tax deductions for large capital expenditures are highly variable and have also been set to zero. These incentives can be easily included when performing a detailed analysis for a particular location. In vast majority of cases, these incentives will give a cost advantage to the renewable energy power systems.

In the discounted cash-flow cost analysis, discount rates must be used to adjust future costs to net present values. Future values FV are adjusted to present values PV using the following equation [19]:

$$PV = \frac{FV}{(1+i)^x} \tag{3}$$

where i is the discount rate and x is the year in which the future expense occurs. This equation is used for discrete events, such as an inverter replacement after 10 years, or the diesel projected price during year 4.

Operating and maintenance costs are typically presented as uniform annual costs over the system life. Uniform costs are adjusted to net present costs using [19]:

$$P = A\frac{(1+i)^n - 1}{i(1+i)^n} \tag{4}$$

where A is the annual cost, i is the discount rate, and n is the system lifetime in years.

3. System models

3.1. RO system

3.1.1. Physical model

To limit the computational requirements, a simplified reverse osmosis system model was employed. Instead of determining the size of the reverse osmosis membrane array and calculating the energy requirements, average values for seawater reverse osmosis systems are used. Here, the design variable is the system water production capacity and it is assumed that the energy requirements for the reverse osmosis system are given by:

$$E_{RO}(t) = SEC \times V_{RO,\max} \tag{5}$$

where $V_{RO,\max}$ is the maximum volume of water produced by the system per hour in m^3 and SEC is the system specific energy consumption in kWh/m^3. For this analysis, the specific energy consumption is assumed to be 4 kWh/m^3 [20].

3.1.2. Cost model

A simplified model was also used to describe the capital costs of the reverse osmosis system. It was assumed that the capital costs of the reverse osmosis unit can be found using:

$$C_{RO} = V_{RO,\text{maxday}} U_{RO} \tag{6}$$

where $V_{RO,\text{maxday}}$ is the rated daily production of the reverse osmosis system in m^3/d and U_{RO} is the specific system cost in $\$/(m^3/d)$. For the small-scale systems considered here, the specific system cost is assumed to be $\$2{,}400/(m^3/d)$ [21].

The capital cost of the infrastructure to support the reverse osmosis system must also be considered. Here, it is assumed that the infrastructure costs are proportional to the reverse osmosis system costs as shown:

$$C_{\text{infra}} = \varphi_{\text{infra}} C_{RO} \tag{7}$$

where φ_{infra} is proportionality constant between the infrastructure and the reverse osmosis system. For the cases considered here, the proportionality constant is assumed to be 1.71 [22].

The total annual operational cost for the reverse osmosis system is given by:

$$A_{Op,RO} = A_l + A_{\text{chem}} + A_{r,RO} \tag{8}$$

where A_l is the annual labor cost, A_{chem} is the annual chemical cost, and $A_{r,RO}$ is the annual cost of component replacement in \$.

The annual cost of the labor is expressed as:

$$A_l = 365\gamma V_{RO,\text{system}} \tag{9}$$

where γ is the specific operating labor cost in \$/m^3 and $V_{RO,\text{system}}$ is the average daily production in m^3. In this analysis, the nominal labor cost was chosen as \$3.00/m^3 [15].

The chemical costs are also location specific as the pretreatment chemicals are dependent on local water conditions. The total annual cost of treatment chemicals is given by:

$$A_{\text{chem}} = 365 k V_{\text{RO,system}} \tag{10}$$

where k is the average cost of chemicals \$/m^3. In this analysis, the treatment chemical cost per m^3 is assumed to be \$0.033 [21].

Throughout its lifetime, certain components of the reverse osmosis system will require replacement. The major components that will require regular replacement are the reverse osmosis membranes. The components and their percentage of the RO system cost are shown in Table 1 and replacement rates for a typical system are given in Table 2.

Using the replacement rate data in Table 2 and the component costs found in Table 1, the annual cost for component replacement can written as:

$$A_{r,RO} = C_{\text{mem}} RR_{\text{mem}} + C_p RR_p + C_{\text{motor}} RR_{\text{motor}} + C_{er} RR_{er} \tag{11}$$

where C represents the component costs and RR is the component replacement rate.

3.2. Water storage

Water storage is required to ensure that the reverse osmosis system can meet the peak water demand. In addition, it is used as the main storage mechanism for bad weather when batteries are not included the system. Here, it is assumed that the water tanks are available in discrete sizes. Their sizes and capitals costs, C_{tank}, are given in Table 3. There will be simple maintenance required to ensure the tank is clean. Here, it is assumed that the annual tank maintenance (A_{tank}) is \$414 [23].

3.3. Batteries

Batteries are commonly used in renewable energy power systems to deal with intermittency. Here, lead–acid batteries are considered as they are the most common technology used in off-grid renewable energy systems [24]. Energy is lost during the battery charge/discharge cycle. Here, a typical constant charge/discharge efficiency for lead–acid batteries of 85% is used [25].

A modified rainflow battery model is used to determine the battery life [26]. In this model, the number of cycles to failure determines the battery life. The number battery charge/discharge cycles to failure depends on the current state of battery charge while discharging. If discharging from full battery pack capacity, the number of cycles to failure is given by:

Table 1
Simulation model framework [22]

System component	Contribution to capital costs
Intake cost	25% of system capital costs
Pretreatment system	10% of system capital costs
Reverse osmosis components	25% of system capital costs
Post-treatment & brine disposal	5% of system capital costs
Installation & infrastructure	30% of system capital costs
Professional costs	5% of system capital costs

Table 2
Replacement rates for reverse osmosis components [15]

Component	Cost	Annual replacement rate (%)
Membranes	40% of RO components	20
Pumps	15% of RO components	10
Motors	15% of RO components	10
Energy recovery devices	15% of RO components	10

Table 3
Water storage costs [23]

Size	Cost
5	$3,963
10	$6,163
15	$9,045
20	$10,645
30	$14,007
40	$17,208
50	$17,448

Table 4
Lead acid battery constants [23]

Constant	Value
a_1	1380.3
a_2	6833.5
a_3	8.750
a_4	6746.5
a_5	6.216
b_{LC}	0.5

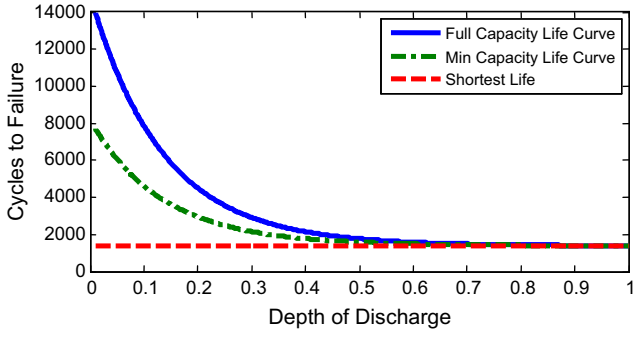

Fig. 3. Battery failure curve.

$$F_{C,i} = a_1 + a_2 e^{-a_3 R_i} + a_4 e^{-a_5 R_i} \tag{12}$$

where the a_i are battery constants as given Table 4. A sample full capacity life cycle curve is shown in Fig. 3.

If discharging from the bottom of the battery, the number of cycles to failure is given by:

$$F_{CL,i} = b_{LC}\left(F_{C,i} - F_{CR}\right) + F_{CR} \tag{13}$$

where F_{CR} is the asymptotic shortest life on the failure curve in Fig. 3 and b_{LC} is the lifecycle adjustment factor (between 0 and 1).

In the battery simulation, the mean state of charge, $m_{bat,i}$ and range of discharge, R_i are recorded for each battery cycle. The number of cycles to failure for a cycle range and mean capacity is estimated using:

$$\widehat{F}_{C,i} = F_{C,i} - \left(F_{C,i} - F_{CL,i}\right)\frac{1 - R_i/2 - m_{bat,i}/E_{bat,cap}}{1 - R_i} \tag{14}$$

where $E_{bat,cap}$ is the battery pack storage capacity. The lifetime of the batteries is determined using:

$$L_{bat} = \frac{n_{years}}{\sum_{i=1}^{n_{cycles}} 1/\widehat{F}_{C,i}} \tag{15}$$

where n_{years} is the number of years in the system simulation and n_{cycles} is the number of battery cycles.

The estimated capital and operating costs for the batteries are detailed below. The capital cost for the lead–acid battery system including control electronics is given by [25]:

$$C_{bat,cc} = C_{bat,power} + C_{bat,storage} + C_{bat,BOP} \tag{16}$$

where $C_{bat,power}$ is the cost associated with maximum battery power output, $C_{bat,storage}$ is the cost associated with the capacity of the battery pack, and $C_{bat,BOP}$ is the cost of the balance of plant components. These values are given by:

$$\begin{aligned} C_{bat,power} &= 125 P_{sys} \\ C_{bat,BOP} &= 150 E_{bat,cap} \end{aligned} \tag{17}$$

where P_{sys} is the battery pack maximum power output.

The lifetime of lead–acid batteries is limited and the estimated replacement costs are given by [25]:

$$C_{bat,rc} = 150E_{bat,cap} \tag{18}$$

Finally, battery pack maintenance is also required and is estimated using the following relationship [25]:

$$C_{bat,OM} = 15P_{sys} \tag{19}$$

3.4. Diesel generator

3.4.1. Physical model

The diesel generator model was developed using data from [27]. The engine can work at any power output between zero and its maximum rating. The maximum mechanical efficiency, obtained at the maximum rating, is set to 35%, an average value for modern engines. This is then multiplied by the assumed alternator efficiency of 80%. In these cases, the diesel generator capacity is the design variable and it is assumed here that the diesel generator always runs at full capacity. A lower heating value of 35 MJ/L is assumed for the diesel. The final generator behavior is shown in Fig. 4 and the efficiency is independent of generator size.

3.4.2. Cost model

The capital and operating costs of diesel generators are estimated as follows [27]:

$$\begin{aligned} C_{gen,cc} &= 3,300 \times S^{0.605} \\ C_{gen,OM} &= N(0.207 + 0.211\,S) \end{aligned} \tag{20}$$

where N is the number of operating hours and S is the engine size.

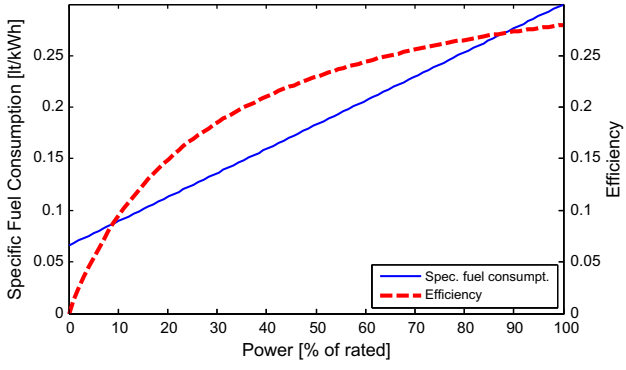

Fig. 4. Diesel fuel use and efficiency.

Fuel is a significant component of the lifecycle cost for the diesel-powered reverse osmosis systems. In this work, price projections from the Energy Information Administration are used to estimate the cost of the diesel fuel over the system life [28]. Costs are adjusted to the net present value. The price is also increased by 0.20 $/L to account for transportation to the remote area. Fig. 5 shows the price projection.

3.5. Wind

3.5.1. Physical model

The wind turbine system optimized here (see Fig. 6) consists of a turbine driving an electrical generator mounted on top of a self-supported lattice tower. The wind generator charges batteries, if present, and powers the reverse osmosis unit. The design variables for the wind reverse osmosis optimization problem are the number of turbines, the type of turbine, the height of the turbine in m, the size of the batteries in kWh, the production capacity of the reverse osmosis system in m^3/d, and the size of the water storage system.

The turbine power output is calculated for the wind profile. The NOAA Satellite and Information Service was used to obtain data for each location [29]. This wind speed data is from a height of 10 meters. Since the tower height can vary, the expected wind speed for a given system is scaled appropriately using [30]:

$$V = V_0\left(\frac{H}{H_0}\right)^{\alpha} \tag{21}$$

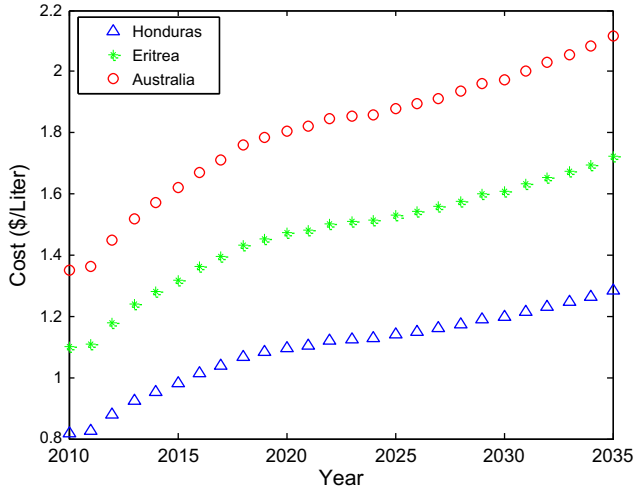

Fig. 5. Projected diesel fuel costs.

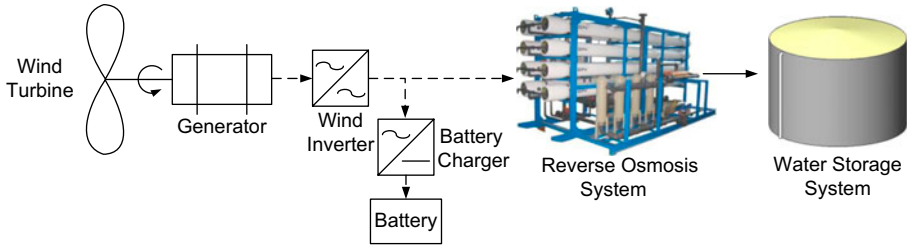

Fig. 6. Wind-powered reverse osmosis system.

where V_0 is the measured wind speed, H_0 is the height at which the wind speed was measured (10 m), H is the hub height of the turbine (tower height), and α is a constant. It is assumed that there is no vegetation at the site and α has a value of 1/7 [30].

With the scaled wind speed, the power output is determined for a given turbine from its characteristic power output curve. The power output curve for the Gaia Wind 133–11 kW is shown in Fig. 7. It exhibits a speed below which no power is produced and a speed above which the system blades must be feathered to reduce loads.

3.5.2. Cost model

Candidates for the wind turbine generation system are presented in Table 5. The costs include both the turbines and generators. Tower and wiring costs are determined based on manufacturer's pricing [33–35]. The costs are given by:

$$C_{Twr} = 23.23H^2 + 175.2H + 85$$
$$C_{WR} = 13.482H + 835.15 \quad (22)$$

where H is the tower height in m. Installation costs are determined using [34]:

$$C_{Inst} = 0.3(C_{WG} + C_{Twr} + C_{WR}) \quad (23)$$

where C_{WG} is the cost of the wind turbine and generator. The total capital costs are therefore:

$$C_{W,cc} = C_{WG} + C_{Twr} + C_{WR} + C_{Inst} \quad (24)$$

The annual operating and maintenance costs for the wind turbines are found using [30]:

$$A_{W,OM} = 0.02C_{W,cc} \quad (25)$$

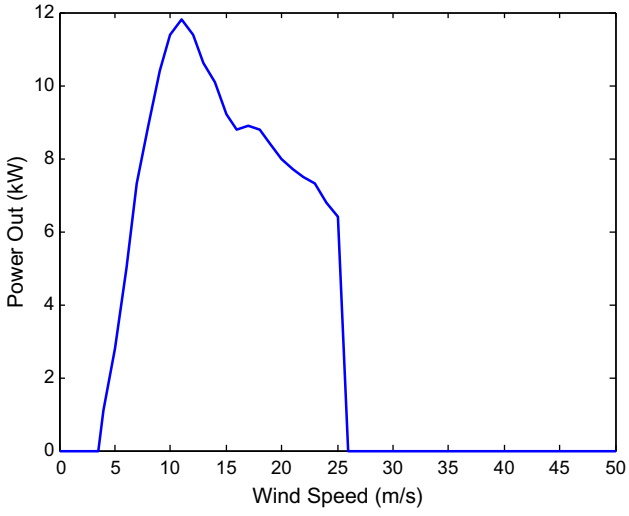

Fig. 7. Power output curve for Gaia Wind 133–11 kW turbine.

3.6. Photovoltaics

3.6.1. Physical model

The photovoltaic-powered reverse osmosis system optimized here (see Fig. 8) consists of a photovoltaic panel, batteries, supporting electronics, a reverse osmosis system, and water storage. The photovoltaic panel charges batteries, if present, and powers the reverse osmosis unit. The design variables for the PVRO optimization problem are the area of PV panels in m, the size of the batteries in kWh, the production capacity of the reverse osmosis system in m^3/d, and the size of the water storage system in m^3.

For the cases conducted here, the energy produced by the photovoltaic system in one hour at time step t is written as:

$$E_{Solar}(t) = \eta_{mppt}\eta_{pv}G(t)A_{pv}\Delta t \quad (26)$$

Table 5
Selected commercially available wind turbines

Turbine	Generator rating (kW)	Cut-in speed* (m/s)	Cut-out speed** (m/s)	Retail price (USD)
Bergey Excel-R/48 [31]	7.5	3.1	15.6	24,750
Gaia Wind 133–11 kW [32]	11	3.5	25	46,000
Alize [31]	10	3.1	25	31,100
Halus V-17 [31]	75	3.1	30	110,000

*Wind speed at which power production starts.
**Maximum wind speed at which power is produced before furling.

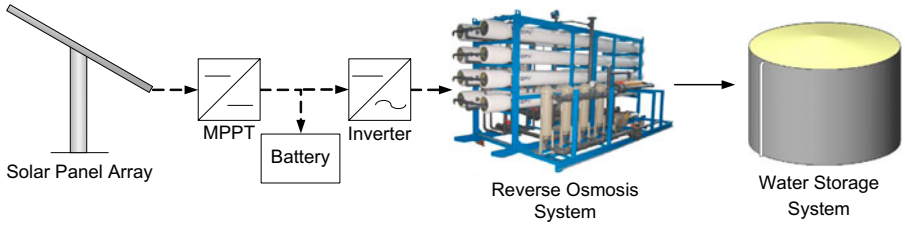

Fig. 8. Photovoltaic-powered reverse osmosis system.

where η_{mppt} is the efficiency of the maximum power point tracker, η_{pv} is the efficiency of the photovoltaic panel, $G(t)$ is the solar radiation in kW/m^2 at time t, A_{pv} is the solar array area in m^2, and Δt is the size of the time step (1 h). Silicon PV panels are considered with an efficiency of 15% [36] and the maximum power point tracker has an assumed efficiency of 98% [36].

3.6.2. Cost model

The installed capital cost of the PV portion of the system was estimated using the following relationship:

$$C_{pv,cc} = 1000 U_{pv} \eta_{pv} A_{pv} \quad (27)$$

where U_{pv} is the cost of the installed system in \$/W$_p$. This value was assumed to be \$5.00/W$_p$ based on published costs from small photovoltaic power systems [37]. Due to the 25-year guaranteed life of the PV panels, the system electronics are the only components that are assumed to require replacement. The PV electronics cost is given by [37]:

$$C_{pv,rc} = 0.07 C_{pv,cc} \quad (28)$$

The electronics replacement rate was assumed to be seven years. The operating and maintenance costs were also estimated using compiled data from small-scale PV systems [37]:

$$C_{pv,OM} = 0.015 C_{pv,cc} \quad (29)$$

3.7. Hybrid system

It has been shown in the studies of power systems that their costs can be reduced by combining technologies to form a hybrid system [38]. This happens for several reasons. First, winds tend to be stronger during the winter, while solar radiation tends to be stronger during the summer. Second, diesel generators can operate as a backup when solar or wind energy is not sufficient. This operating mode can drastically reduce the battery size.

The hybrid system considered is shown in Fig. 9. The design variables for this configuration include the type of wind turbines, the number of wind turbines, the area of solar panels in m^2, the battery capacity in kWh, the capacity of the diesel generator in kW, the generator control variables (described below), the capacity of the reverse osmosis system in m^3/d, and the volume of the storage in m^3. As in the previous cases, the respective power sources are used to charge the batteries, which are in turn used to run the reverse osmosis system. The system produces water that is stored in a water tank for consumption by the community.

The performance of the system is highly affected by how it is controlled. In this case, when to turn on and off the diesel generator are the control variables.

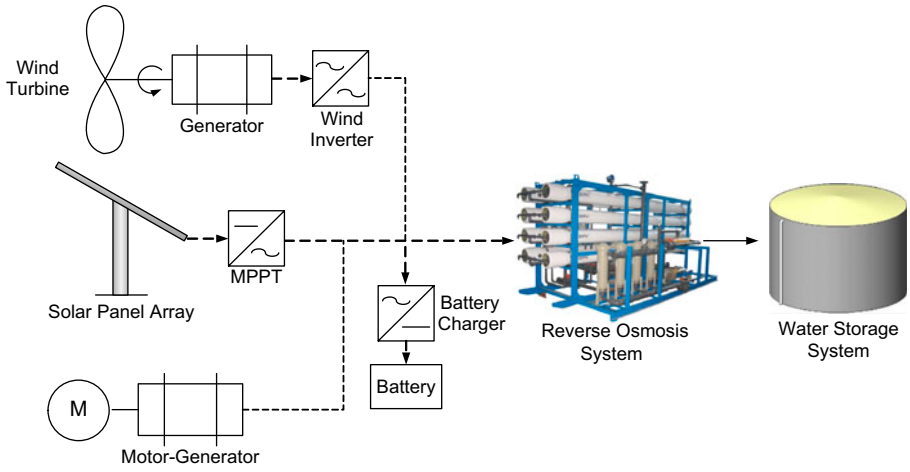

Fig. 9. Hybrid-powered reverse osmosis system.

Here, the engine is started when the battery charge decreases below the lower threshold, and is stopped when the charge goes above the upper threshold. This behavior is pictured in Fig. 10. The thresholds are treated as design variables by the optimizer.

4. System models

4.1. Study description

Here, the method is applied to the design of a reverse osmosis system for a small community. It is assumed that the community has 200 residents that require 50 L/person/d, which is an adequate amount of water for drinking and other basic needs [39]. It is assumed that all the water is withdrawn from the storage during the day, with a withdrawal profile as seen in Fig. 11. Any profile can be used in this approach, but this basic profile was selected for simplicity. It is also assumed that the system operates for 24 h a day. This can be easily changed to limited use in the architecture above.

Systems were designed for three locations to show the range of possible solutions. The locations selected are Nuova Octopeque in Honduras, Massawa in Eritrea, and Broome in Australia. The water requirements and power requirements for reverse osmosis are assumed to be independent of location, but the wind speed, solar radiation, and fuel price are location dependent. These differences will influence the system design.

The following energy technologies are considered: solar photovoltaic panels, wind turbines, and IC diesel generators. Battery energy storage is included when using solar or wind power. A hybrid system using all three technologies is also analyzed. For each choice of

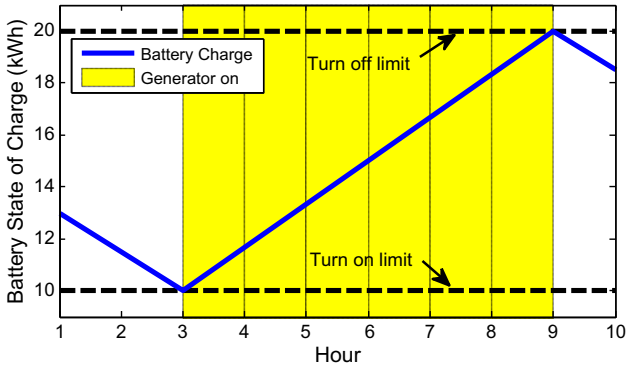

Fig. 10. Generator control variables.

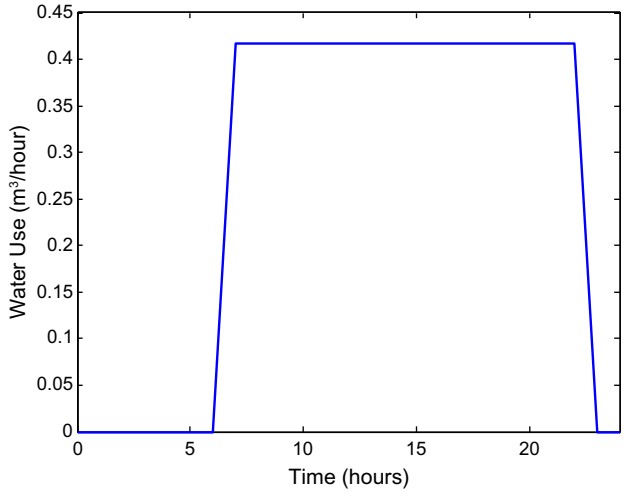

Fig. 11. Water use profile for case studies.

energy source, a reverse osmosis system is configured that meets the *LOWP* requirement. The absence of water can have large consequences and here the reverse osmosis systems are designed to have a *LOWP* smaller than 1%.

Any system design satisfying the *LOWP* is adequate to provide water to the community. However, the most practical configuration has the lowest lifetime cost. Total system cost is comprised of the capital cost and the yearly costs of maintenance and fuel. The system is assumed to run for 25 years, and the costs in following years are discounted at a rate of 5%, which is the assumed difference between the inflation rate and the bank interest rate.

4.2. Diesel reverse osmosis system

The diesel-powered reverse osmosis systems designed for the sample locations are presented in Table 6. Since the system is assumed to run 24 h a day and the reverse osmosis model is simplified to assume the same power requirements for all locations, the system configurations are the same. All of the system configurations are composed of a 10 m^3/d reverse osmosis system, a 1.7 kW generator, and a 5 m^3 water storage tank. The main difference in cost is the variation in fuel prices by location. In the baseline year of 2010, the fuel prices ranged from \$0.82 in Honduras to \$1.35 in Australia. As a result, the most economic configuration for the diesel-powered system is in Honduras at a net present cost of \$397,100.

4.3. Wind reverse osmosis system

Wind-powered reverse osmosis systems (see Fig. 6) for each location are presented in Table 7. The significant change from the diesel-powered configuration is that all wind systems store water instead of using batteries. This is due to the relatively high availability of the wind resource. The system costs range from \$530,400 for Honduras, which has the best wind resource, to \$558,300 for Australia, which has the lowest average wind speed. Although the system costs have been optimized, they are still higher than the corresponding diesel-powered reverse osmosis systems. This is due to the high costs of the wind and reverse osmosis equipment, which needs to be oversized to deal with the variability of the wind resource. The costs associated with the small-scale wind turbines or reverse osmosis systems would need to be

Table 6
Diesel-powered reverse osmosis details

Configuration	Honduras	Eritrea	Australia
Reverse osmosis system size (m^3/d)	10	10	10
Diesel generator size (kW)	1.7	1.7	1.7
Water storage size (m^3)	5	5	5
Capital cost (k\$)	73.5	73.5	73.5
Net present O&M and replacement cost (k\$)	233.0	233.0	233.0
Net present fuel cost (k\$)	90.6	103.7	124.3
Total net present cost (k\$)	397.1	410.2	430.8

Table 7
Wind-powered reverse osmosis details

Best configuration	Honduras	Eritrea	Australia
Reverse osmosis system size (m^3/d)	23.1	21.6	25.4
Water storage size (m^3)	50	50	50
Number of turbines	1	1	1
Turbine power rating (kW)	11	11	11
Turbine height (m)	30.3	42.1	30.1
Battery capacity (kWh)	0	0	0
Battery life (years)	N/A	N/A	N/A
Capital cost (k\$)	251.5	257.9	268.6
Net present O&M and replacement cost (k\$)	279.0	276.2	289.7
Total net present cost (k\$)	530.4	534.1	558.3

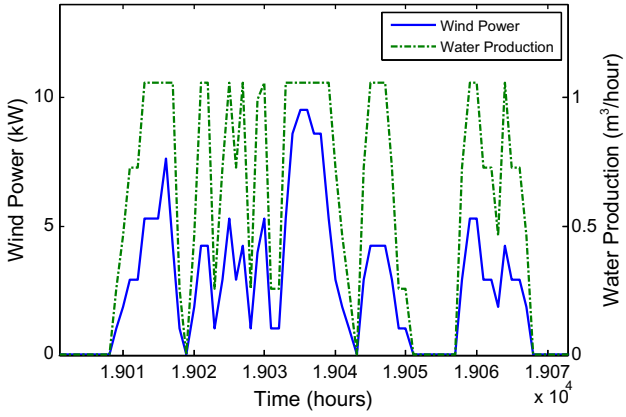

Fig. 12. Wind power output and water production for Australia system over a three-day period.

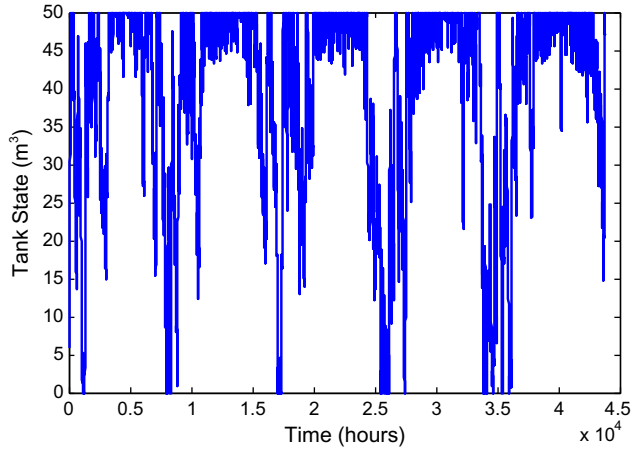

Fig. 13. Water storage over five-year period in Australia system.

reduced to make these configurations competitive with the diesel-powered reverse osmosis systems.

The simulated performance of the Australian wind-powered reverse osmosis system can be seen in Figs. 12 and 13. Fig. 12 displays the instantaneous wind power and corresponding water production for the batteryless system. The production varies according to the wind power output until it saturates at the system capacity. The resulting water stored in the tank is shown for the entire five-year period in Fig. 13. It can be seen that there are a few instances where the tank is empty, matching the requirement that the loss of water probability be less than 1%. This LOWP constraint can be varied if there is no backup water source available to make the system more reliable at a higher system cost.

4.4. PVRO system

The solar-powered reverse osmosis configurations are presented in Table 8. These cases have incorporated battery energy storage because the energy for the solar case comes in over a smaller period of time than the wind energy. If the solar-powered RO systems do not use batteries, the RO units must be larger to produce enough water in a shorter time period. For the test cases, using a larger reverse osmosis system is not as cost effective as spreading out the production with a smaller reverse osmosis system with batteries.

The system costs range from $390,800 for Honduras to $403,300 for Eritrea. The photovoltaic-powered reverse osmosis systems are more cost effective than their wind and diesel-powered equivalents. The rapidly dropping costs of photovoltaics make PVRO systems applicable to a wide range of locations despite the seasonal and daily variability.

Simulated performance of the optimized Honduras PVRO system can be seen in Figs. 14 and 15. Fig. 14 shows the performance of the energy system over a 10-d period. There is a daily cycling of the battery pack and the batteries reach their maximum charge on

Table 8
Photovoltaic-powered reverse osmosis details

Best configuration	Honduras	Eritrea	Australia
Reverse osmosis system size (m^3/day)	10.5	10.5	10.7
Water storage size (m^3)	5	15	50
PV area (m^2)	76.0	82.2	71.2
Battery capacity (kWh)	31.1	30.0	24.0
Battery life (Years)	4.1	4.0	3.9
Capital cost (k$)	149.7	158.2	158.4
Net present O&M and replacement cost (k$)	241.1	245.1	242.6
Total net present cost (k$)	390.8	403.3	400.9

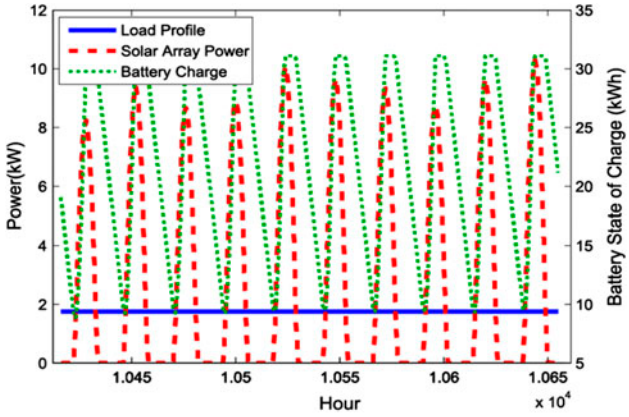

Fig. 14. Water storage over 50-day period in Honduras.

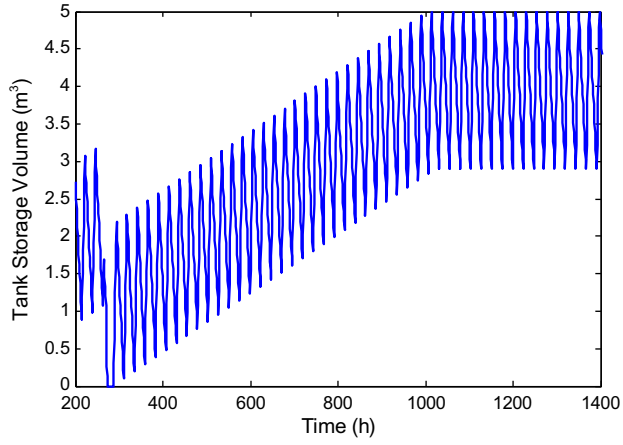

Fig. 15. Water storage over 50-day period in Honduras.

a typical day. Fig. 15 shows the behavior of the water in storage over a 50-d period. It can be seen that after a period of bad weather, the system slowly recovers to the full tank condition. This slow recovery occurs because the reverse osmosis system only provides an extra 0.5 m^3 of water per day.

4.5. Hybrid system

Hybrid-, diesel-, wind-, and solar-powered reverse osmosis systems (see Fig. 9) for the three locations are presented in Table 9. All three cases include different mixes of energy sources. The Honduras system is a pure photovoltaic power system, Eritrea system is a photovoltaic/diesel generator hybrid, and the Australia system is a wind/photovoltaic hybrid system. All of the configurations include photovoltaics, as all locations have good solar resources. The costs for all systems are very similar: between $390,800 and $396,100.

The simulated performance for the Eritrea system can be seen in Figs. 16 and 17. Fig. 16 shows the power system operation for the hybrid diesel/solar system. For the days shown, the solar radiation was not strong, so the diesel generator turned on to supplement the solar energy. The diesel generator ensures that the batteries are never completely drained, and the system is able to operate at constant set point. This is reflected in the amount of water in storage shown in Fig. 17. During the daytime, the water in the storage drops as it is used and it is refilled by the system in the evening.

Table 9
Hybrid-powered reverse osmosis details

Best configuration	Honduras	Eritrea	Australia
Reverse osmosis system size (m^3/day)	10.5	10.5	10.9
Water storage size (m^3)	5	5	20
PV area (m^2)	76.0	51.8	27.3
Generator size (kW)	0	5.2	0
Generator turn on (kWh)	N/A	12.3	N/A
Generator turn off (kWh)	N/A	30.2	N/A
Number of turbines	0	0	1
Turbine power rating (kW)	N/A	N/A	8
Turbine height (m)	N/A	N/A	21.9
Battery capacity (kWh)	31.1	51.7	28.7
Battery life (Years)	4.1	5.5	5.6
Capital cost (k$)	149.7	143.9	156.9
Net present O&M and replacement cost (k$)	241.1	252.2	237.1
Total net present cost (k$)	390.8	396.1	394.0

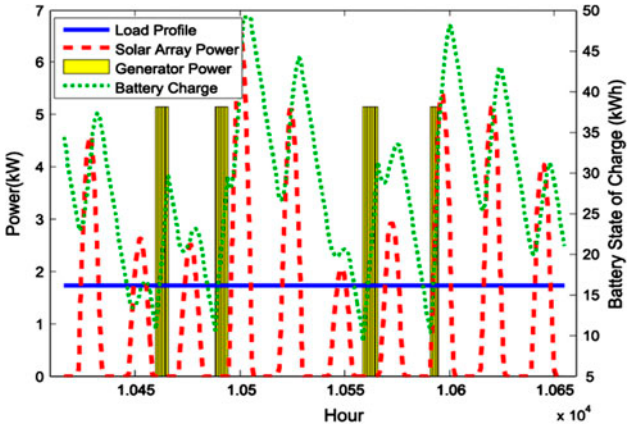

Fig. 16. Power system performance over 10-day period in Eritrea system.

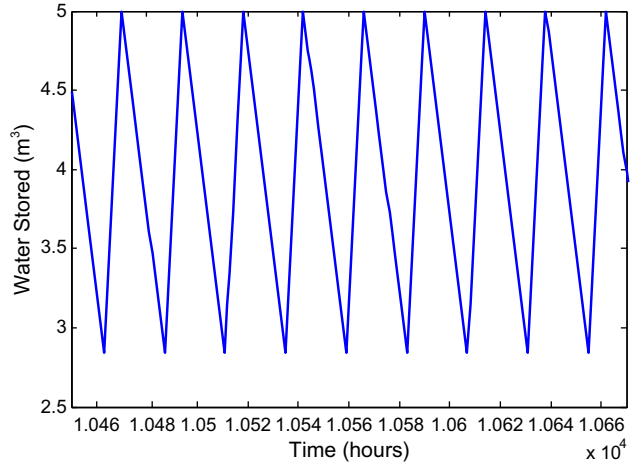

Fig. 17. Water storage over 10 day period in Eritrea system.

5. Summary and conclusions

This paper presents a method to guide the design of power systems for reverse osmosis in remote communities. The method compares the economics of reverse osmosis and power system combinations to determine the lowest cost solution for a specified location and water demand. The following energy sources are considered: photovoltaic arrays, wind turbines, diesel generators, a storage element such as lead–acid batteries, and any hybrid system combination. In addition, the method sizes the reverse osmosis system and water storage tank.

The method determines the size of the elements that minimize the lifetime cost of the off-grid reverse osmosis system while meeting the community water demand with a specified probability. Optimization methods are coupled with simulation models. These models use capital and maintenance costs to determine the total system cost, and site-specific hourly solar and wind data for a five-year period to determine if the system is able to meet the water requirements of a given community.

The method is demonstrated by configuring reverse osmosis systems for communities near Nueva Octopeque in Honduras, Massawa in Eritrea, and Broome in Australia. In all cases, the method is used to design a water system which provides 10 m^3 of water per day, a suitable amount for a community of 200 people. Results show that, for a single power source small-scale reverse osmosis system, the photovoltaic technology is at the moment superior to wind turbines and diesel generators, wherever the insolation is relatively constant. Nevertheless, hybrid-powered reverse osmosis systems are more cost effective in Eritrea and Australia. In Eritrea, photovoltaics combined with a diesel generator offers the best performance by balancing the volatility of the intermittent power sources when needed. In Australia, the profiles of the wind and solar resources complement each other to make a wind and solar hybrid the most cost-effective solution.

These results are consistent with the literature and show that the method is able to use local climatic conditions to configure small-scale, stand-alone reverse osmosis systems. Additional reliability aspects and availability of components should be considered when using this method to design real-world small-scale reverse osmosis systems. With such additions, this method can be easily applied to any location and water requirements to aid in reverse osmosis system design for remote communities.

References

[1] World Health Organization and Unicef, Progress on Sanitation and Drinking Water: 2010 Update, World Health Organization and Unicef, Geneva, 2010.
[2] OECD/IEA, Energy Poverty: How to make modern energy access universal?-Special Early Excerpt of the World Energy Outlook 2010 for the UN General Assembly on the Millennium Development Goals, World Energy Agency, Paris, 2010.
[3] D. Herold, V. Horstmann, A. Neskakis, J. Plettner-Marliani, G. Piernavieja, R. Calero, Small scale photovoltaic desalination for rural water supply—Demonstration plant in Gran Canaria, Renewable Energy 14(1–4) (1998) 293–298.
[4] D. Herold, A. Neskakis, A small PV-driven reverse osmosis desalination plant on the island of Gran Canaria, Desalination 137(1–3) (2001) 285–292.
[5] Spectra Watermakers, 2009, SSW 3500 Datasheet. Available from: http://www.spectrawatermakers.com/documents/Solar_Cube.pdf (February 18, 2010).

[6] E. Tzen, D. Theofilloyianakos, Z. Kologios, Autonomous reverse osmosis units driven by RE sources experiences and lessons learned, Desalination 221(1–3) (2008) 29–36.
[7] E. Tzen, K. Perrakis, P. Baltas, Design of a stand alone PV—Desalination system for rural areas, Desalination 119(1–3) (1998) 327–333.
[8] E. Tzen, D. Theofilloyianakos, M. Sigalas, K. Karamanis, Design and development of a hybrid autonomous system for seawater desalination, Desalination 166 (2004) 267–274.
[9] E.S. Mohamed, G. Papadakis, E. Mathioulakis, V. Belessiotis, A direct coupled photovoltaic seawater reverse osmosis desalination system toward battery based systems—A technical and economical experimental comparative study, Desalination 221(1–3) (2008) 17–22.
[10] A.M. Thomson, Reverse-Osmosis Desalination of Seawater Powered by Photovoltaics Without Batteries, Ph.D., Loughborough University, Loughborough, 2003.
[11] M. Thomson, D. Infield, A photovoltaic-powered seawater reverse-osmosis system without batteries, Desalination 153(1–3) (2003) 1–8.
[12] M. Thomson, D. Infield, Laboratory demonstration of a photovoltaic-powered seawater reverse-osmosis system without batteries, Desalination 183(1–3) (2005) 105–111.
[13] M.S. Miranda, D. Infield, A wind-powered seawater reverse-osmosis system without batteries, Desalination 153(1–3) (2003) 9–16.
[14] A.M. Bilton, R. Wiesman, A.F.M. Arif, S.M. Zubair, S. Dubowsky, On the feasibility of community-scale photovoltaic-powered reverse osmosis desalination systems for remote locations, Renewable Energy 36(12) (2011) 3246–3256.
[15] A.M. Helal, S.A. Al-Malek, E.S. Al-Katheeri, Economic feasibility of alternative designs of a PV-RO desalination unit for remote areas in the United Arab Emirates, Desalination 221(1–3) (2008) 1–16.
[16] D. Voivontas, K. Misirlis, E. Manoli, G. Arampatzis, D. Assimacopoulos, A tool for the design of desalination plants powered by renewable energies, Desalination 133(2) (2001) 175–198.
[17] K. Bourouni, T. Ben M'Barek, A. Al Taee, Design and optimization of desalination reverse osmosis plants driven by renewable energies using genetic algorithms, Renewable Energy 36(3) (2011) 936–950.
[18] T. Ben M'Barek, K. Bourouni, K.B. Ben Mohamed, Optimization coupling RO desalination unit to renewable energy by genetic algorithms, Desalin. Water Treat. 51(7–9) (2012) 1416–1428.
[19] J. White, K. Case, D. Pratt, Principles of Engineering Economic Analysis, Wiley Higher Education, Hoboken, NJ, 2010.
[20] M. Li, Reducing specific energy consumption in reverse osmosis (RO) water desalination: An analysis from first principles, Desalination 276(1–3) (2011) 128–135.
[21] H.M. Ettouney, H.T. El-Dessouky, R.S. Faibish, P.J. Gowin, Evaluating the economics of desalination, Chem. Eng. Prog. 12 (2002) 32–38.
[22] A. Hafez, S. El-Manharawy, Economics of seawater RO desalination in the Red Sea region, Egypt. Part 1. A case study, Desalination 153(1–3) (2003) 335–347.
[23] L. Domènech, D. Saurí, A comparative appraisal of the use of rainwater harvesting in single and multi-family buildings of the Metropolitan Area of Barcelona (Spain): Social experience, drinking water savings and economic costs, J. Cleaner Prod. 19(6–7) (2011) 598–608.
[24] M. Perrin, Y.M. Saint-Drenan, F. Mattera, P. Malbranche, Lead–acid batteries in stationary applications: Competitors and new markets for large penetration of renewable energies, J. Power Sources 144 (2005) 402–410.
[25] S.M. Schoenung, W.V. Hassenzahi, Long-vs. Short-Term Energy Storage Technologies Analysis—A Life-Cycle Cost Study, Sandia National Laboratories, Alburquerque, NM, 2003.
[26] J.F. Manwell, J.G. McGowan, U. Abdulwahid, K. Wu, Improvements to the Hybrid 2 Battery Model, American Wind Energ Association Windpower 2005 Conference, American Wind Energy Association, Denver, CO, 2005.
[27] M. Muselli, G. Notton, A. Louche, Design of hybrid-photovoltaic power generator, with optimization of energy management, Sol. Energy 65(3) (1999) 143–157.
[28] S. Diaf, D. Diaf, M. Belhamel, M. Haddadi, A. Louche, A methodology for optimal sizing of autonomous hybrid PV/wind system, Energy Policy 35(11) (2007) 5708–5718.
[29] NOAA Satellite and Information Service, 2010, Climate Data Online, NOAA Satellite and Information Service, National Climate Data Center, U.S. Department of Commerce. Available from: http://www7.ncdc.noaa.gov/CDO/cdo (May 7, 2010).
[30] P. Gipe, Wind Power for Home & Business. Chelsea Green Publishing Company, White River Junction, VT, 1993.
[31] M. Sagrillo, I. Woofenden, 2010, 2010 Wind Generator Buyer's Guide, Home Power, Home Power, Inc., Ashland, OR, 2010, pp. 44–54. Available from: http://homepower.com/home/ (February 19, 2010).
[32] Gaia-Wind, 2009, Gaia-Wind 133-11kW Data Sheet, Gaia-Wind, Ltd, UK. Available from: http://www.gaia-wind.co.uk (May 7, 2010).
[33] Ampair, 2009, Ampair Price List, Ampair MicroWind, Boost Energy Systems Ltd, UK, p. 4. Available from: http://www.ampair.com/ampair/resources_downloads.asp. (May 7, 2010).
[34] Bergey WindPower, 2010, Bergey Wind Website. Available from: http://www.bergey.com/.
[35] California Energy Commission, 2002, Economics of Owning and Operating DER Technology, Web page.
[36] D. Roche, A. Schinckel, J. Storey, C. Humphris, M. Guelden, Speed of Light: The 1996 World Solar Challenge, UNSW Photovoltaics Special Research Center, Sydney, Australia, 1997.
[37] G. Barbose, N. Darghouth, S. Weaver, R. Wiser, 2013, Tracking the Sun VI; The Installed Cost of Photovoltaics in the United States from 1998 to 2012. Available from: http://emp.lbl.gov/sites/all/files/lbnl-6350e.pdf (March 14, 2014).
[38] M.A. Elhadidy, Performance evaluation of hybrid (wind/solar/diesel) power systems, Renewable Energy 26(3) (2002) 401–413.
[39] G. Howard, J. Bartram, Domestic Water Quantity, Service Level and Health, World Health Organization, Geneva, 2003.